ACS APPLIED MATERIALS & INTERFACES

Research Article

www.acsami.org

Plasmonic Nanosensors for the Determination of Drug Effectiveness on Membrane Receptors

Rubén Ahijado-Guzmán,*[,†] Julia Menten,[†] Janak Prasad,[†,‡] Christina Lambertz,[†] Germán Rivas,[§] and Carsten Sönnichsen*[,†]

[†]Institute of Physical Chemistry, University of Mainz, Duesbergweg 10-14, D-55128 Mainz, Germany

[‡]Graduate School Materials Science in Mainz, Staudingerweg 9, D-55128 Mainz, Germany

[§]Centro de Investigaciones Biológicas, Consejo Superior de Investigaciones Científicas, c/Ramiro de Maeztu 9, 28040 Madrid, Spain

Supporting Information

ABSTRACT: We demonstrate the potential of the NanoSPR (nanoscale surface plasmon resonance sensors) method as a simple and cheap tool for the quantitative study of membrane protein−protein interactions. We use NanoSPR to determine the effectiveness of two potential drug candidates that inhibit the protein complex formation between FtsA and ZipA at initial stages of bacterial division. As the NanoSPR method relies on individual gold nanorods as sensing elements, there is no need for fluorescent labels or organic cosolvents, and it provides intrinsically high statistics. NanoSPR could become a powerful tool in drug development, drug delivery, and membrane studies.

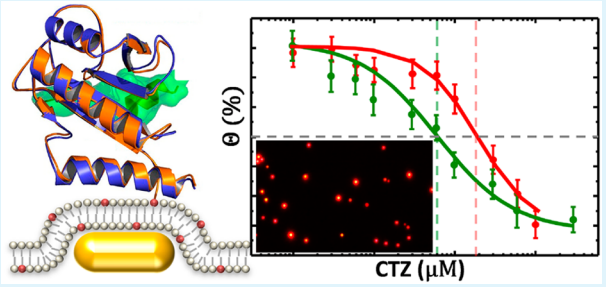

KEYWORDS: *NanoSPR, plasmonic nanosensors, optical dark-field spectroscopy, protein−membrane receptor interactions, drug effectiveness, FtsZ inhibitors*

1. INTRODUCTION

Antibiotic resistance is one of the major emerging problems in medicine. Even one of the most prevalent bacteria living in our guts, *Escherichia coli*, only needs to acquire a few genetic elements to become a highly aggressive pathogen and develop antibiotic resistance.[1,2] In a sort-of "arms race" with pathogens, medical chemistry research needs to continuously identify and synthesize potential antibacterial substances. Over half of the currently validated drug substances are specifically designed to target/inhibit the normal interaction between the membrane receptors and their soluble protein partners, which is often at the start of signaling cascades. High-throughput screening assays are used to identify several dozen or even a hundred potential drug candidates for a given protein system which need to be looked at more closely. Among other things, important parameters to quantify regarding drug candidates are the binding affinity as dissociation constant K_D and the drug effectiveness IC_{50}, which quantifies the concentration of inhibitor necessary to reduce to half the membrane receptor−ligand protein reaction rate.[3−5] This task is still laborious and error prone if the protein system involves membrane proteins. Common techniques are analytical ultracentrifugation with the use of lipid bilayer nanodiscs[6] and/or surface plasmon resonance (SPR) biosensors.[7] Many analytical methods require the use of fluorescent dyes, surfactants, organic solvents, enzymes or antibodies—each of which can potentially alter the system under investigation.[5,8,9] We demonstrated recently that NanoSPR provides a promising sensing platform to quantitatively determine the interaction of many protein systems simultaneously and label-free.[10] In NanoSPR, the functionalized gold nanorods (Au NRs) respond to binding events near their surface by a shift in the plasmon resonance wavelength that is read-out on a single-particle level.[11−14] A big advantage of NanoSPR over classical SPR is the ease by which nanosensors are covered by a lipid membrane.

In this work, we demonstrate the usefulness of this approach to study membrane proteins by comparing two strategies: Au NRs functionalized with Ni-NTA groups and Au NRs covered with a supported lipid membrane containing Ni-NTA-functionalized lipids. In both cases, the Ni-NTA functionalization allows the attachment of His-tagged proteins to the receptor. In our case, the receptor is the protein ZipA, and we determine the dissociation constants for its binding to the ligand FtsZ, with and without the presence of the inhibitors CTZ-*wt* (wild type) and CTZ-*mut* (mutant). In such a three binding-partner system, there are two possible ways to determine binding isotherms, either keeping the inhibitor concentration constant or by varying the inhibitor concentration and keeping the ligand concentration constant. The former yields the K_D value as a function of inhibitor concentration, and the latter gives the IC_{50} values. We performed both types of experiments, with and without a lipid membrane covering the nanosensors, and show

Received: November 2, 2016
Accepted: December 15, 2016
Published: December 15, 2016

DOI: 10.1021/acsami.6b14013
ACS Appl. Mater. Interfaces 2017, 9, 218−223

that valuable insight is obtained in a very straightforward way. Thus, NanoSPR provides a simple, fast, and direct route for the quantitative comparison of the drug interactions and their effectiveness in the presence and absence of a membrane. NanoSPR could become a simple standard tool in pharmaceutical and biomedical laboratories, where protein interactions, membrane receptors, and drug effectiveness are studied.

2. RESULTS AND DISCUSSION

Bacterial cell division is an essential process driven by a multiprotein machinery, the divisome, whose main elements are thus a potential target for antibiotics.[15] In *Escherichia coli*, the first molecular assembly of the divisome, the proto-ring, is formed by interaction between the cytoplasmic protein FtsZ, a GTPase ancestor of tubulin, and two membrane-bound proteins, ZipA and FtsA.[16,17] As inhibitors of these essential bacterial division complexes, we use peptides that mimic the FtsZ C-terminal domain, which contains the binding region to both ZipA and FtsA. Specifically, we used two different mutations of the FtsZ C-terminal domain (amino-acids 367–383). These peptides (KEPDYLDIPAFLRKQAD and KRNDWTNIMAFLKKQAD, we called CTZ-*wt* and CTZ-*mut* respectively), were designed to mimic a segment of the C-terminal region of FtsZ to have an enhanced interaction with ZipA, which results in a mutually exclusive competitive inhibitor.[6,18,19]

For the first set of experiments, we used Ni-NTA functionalized gold nanorods (AuNRs@Ni-NTA) as sensors. The functionalization stabilizes the particles sufficiently so that they tolerate the salt present in the protein buffers. Receptor-functionalized gold nanorods (AuNRs@ZipA) are then created in suspension by simply adding a small amount of the His-tagged protein receptors (typically 5 pmol of ZipA) to small aliquots of the AuNRs@Ni-NTA (for around 5 fmol of nanoparticles) stock solution. These functionalized particles were then immobilized on the wall of a microfluidic flow chamber within a microscope to create our sensor substrate (Figure 1a). In a second step, we deposited pure NTA-functionalized Au NRs as control or reference elements (Figure 1a,b). Before and after each particle deposition step, we washed the flow cell generously with buffer to remove unbound particles and proteins. The fact that these steps are performed with the flow cell already in the microscope, allows recording of the position of particles (by taking an image) after each deposition step. The software automatically remembers these positions and, later, groups the recorded sensor responses accordingly.[10,20] The plasmonic gold nanorods react to the binding of macromolecules by a small shift $\Delta\lambda$ in the wavelength of their plasmon resonance (Figure 1c). Our setups record the plasmon resonance shift of hundreds of individual nanosensors separately with a spectral resolution of 0.3 nm, before and after a ligand/inhibitor is added to the system. The shifts are then shown as small crosses for each condition (Figure 1d). They scatter around a mean value as indicated with a thicker dot with error bars (error bars indicate the statistical error of the mean). The scattering is mostly caused by measurement uncertainty (cf. the reference measurement in Figure 1d left column, where no ligand/inhibitor was added).

We start the set of experiments by using ZipA-functionalized particles, without the membrane. Figure 2a compares the binding affinity curves or binding isotherms of the interaction of the ligand FtsZ to ZipA coated sensors under various conditions: The native interaction (blue), in the presence of a

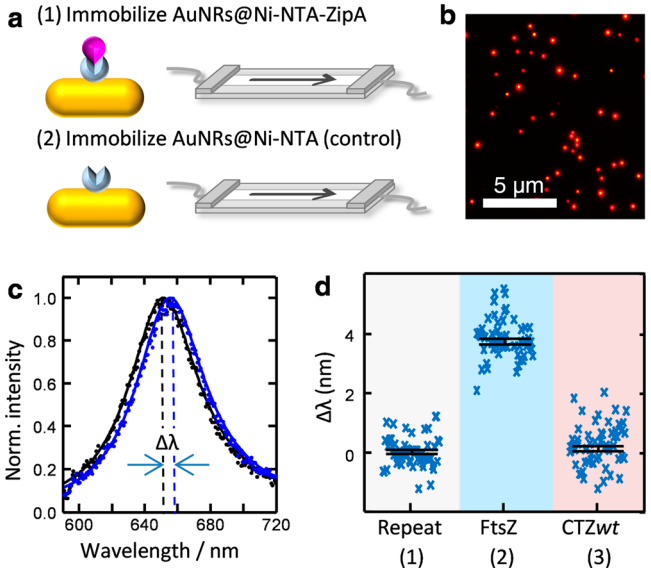

Figure 1. NanoSPR: functionalized nanoparticles, sensor fabrication, and detection principle. (a) Scheme of the flow-cell preparation with immobilized nanoparticles in two steps: (1) with nanoparticles covered by receptor proteins (ZipA) and (2) with nonfunctionalized gold nanorods (AuNRs). (b) Real-color dark-field image of the flow cell showing individual nanoparticles as red dots. The immobilized particles were imaged after each step and systematically assigned to their respective group. (c) The light from every single nanoparticle within the field of view is spectrally resolved before (black) and after (blue) the attachment of the ligand FtsZ. The spectrum shows a plasmon resonance peak that shifts $\Delta\lambda$ after binding of FtsZ to the receptor (ZipA) (d) Our setup records the plasmon shift $\Delta\lambda$ for every particle in the field of view (57 nanoparticles, blue crosses) before and after an analyte is added to the flow cell: (1) with no analyte (to show the repeatability), (2) adding FtsZ, and (3) adding CTZ-*wt* in the presence of FtsZ. The black dots with error bars are the mean values and their standard error.

constant concentration (0.05 μM) of the inhibitors CTZ-*wt* (red) and CTZ-*mut* (green), and, as a control experiment, the interaction for sensors without ZipA functionalization (black).

To determine the binding parameters, we used the Hill equation ($\Delta\lambda/\Delta\lambda_{max} = [FtsZ]^n/K_D + [FtsZ]^n$) (with the coverage $\Theta = \Delta\lambda/\Delta\lambda_{max}$) as fitting function.[21,22] The Hill coefficient "n" describes the cooperativity of the binding process ($n > 1/n < 1$ means positive/negative cooperativity). The native FtsZ-ZipA interaction (blue) shows a K_D value of 5.3 ± 0.5 μM and a Hill coefficient n of 1, resembling absence of cooperativity. K_D values in the presence of the inhibitors CTZ-*wt* (K_D = 33.0 ± 6.1 μM) and CTZ-*mut* (K_D = 25.2 ± 3.0 μM) are very similar but around 1 order of magnitude higher (decreasing the binding affinity) compared to the native interaction. The apparent reduced binding affinity of FtsZ to ZipA is caused by competition with the inhibitors, which is described as the Cheng–Prusoff shift.[23,24] The Hill coefficients (CTZ-*wt* (n = 2.0 ± 0.6) and CTZ-*mut* (n = 1.7 ± 0.3) show a transition to a more cooperative binding process with respect to the native interaction.

For the competition assays (Figure 2b), we use a constant concentration (10 μM) of FtsZ in the flow cell that corresponds to a fraction of around 65% ligand–receptor complexes (See Figure 2a). Now, we increase the concentration of the inhibitors step by step (from 0.01 μM to 100 μM) replacing the FtsZ with increasing concentration. The resulting

DOI: 10.1021/acsami.6b14013
ACS Appl. Mater. Interfaces 2017, 9, 218–223

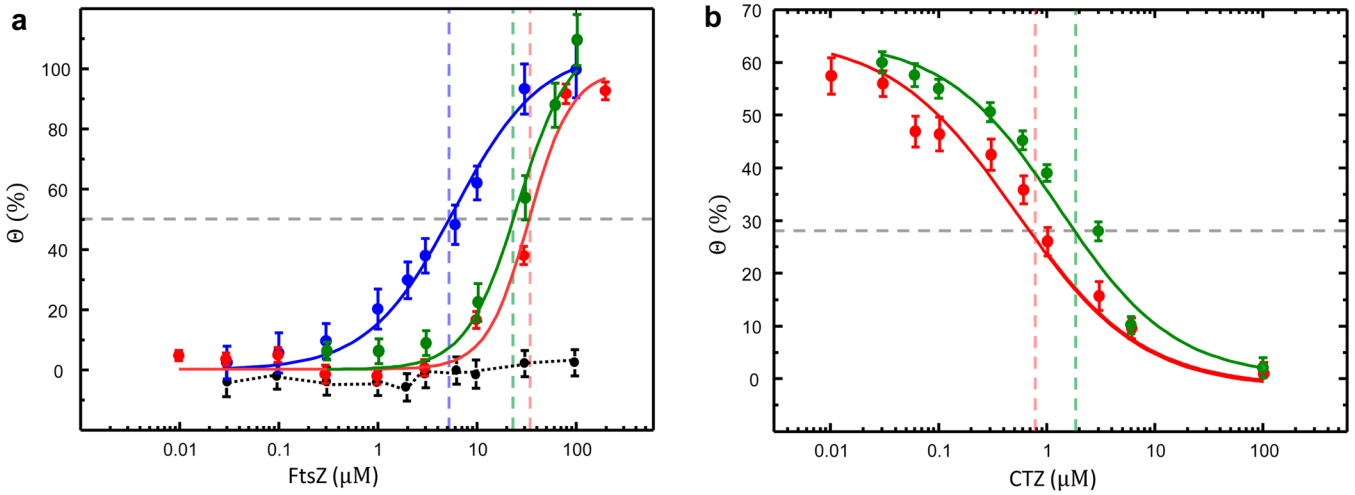

Figure 2. Binding isotherms and competition assay. (a) Binding isotherms of the ligand FtsZ to ZipA-coated nanosensors (blue). Each dot shows the mean and standard error of approximately 40−90 particles, the solid lines are the best fit to the Hill equation, and the dashed lines correspond to the K_D values. The binding isotherms of FtsZ to ZipA shift to higher concentrations (lower affinity) in the presence of the inhibitor peptides CTZ-*wt* (red) and CTZ-*mut* (green). The nonfunctionalized control particles show no unspecific interaction with FtsZ (black). (b) For the competition assays in the absence of a membrane, we increase (titrate) the concentration of the inhibitor peptide CTZ-*wt* (red) and CTZ-*mut* (green) keeping the concentration of FtsZ constant (10 μM). This FtsZ concentration corresponds to approximately 65% of the maximum sensor coverage. The dashed lines correspond to the IC_{50} values.

"negative binding isotherm" is used to obtain the IC_{50} values using the model described in ref.[24] The IC_{50} value corresponds to the concentration of inhibitor necessary to reduce the apparent FtsZ-ZipA reaction strength by one-half. Here, we obtained for CTZ-*wt* (red) an IC_{50} value of IC_{50} = 0.8 ± 0.2 μM and for CTZ-*mut* (green) a slightly larger value of IC_{50} = 2.0 ± 0.4 μM. This result implies that, in these conditions, CTZ-*wt* is around twice more effective as inhibitor than CTZ-*mut*.

For the second set of experiments, we simply immobilized nonfunctionalized gold nanorods directly from synthesis in our flow-cell and deposited a lipid bilayer containing DGS-NTA-Ni lipids on top of them. After flushing with a solution containing ZipA, each sensor is covered by a membrane containing dozens of ZipA molecules as receptors (Figure 3). A disadvantage of this approach is that all particles are functionalized in the same way so that the control needs to be done as an independent experiment (skipping the protein receptor (ZipA) functionalization step).

Again, we start by adding increasing concentrations of the ligand FtsZ to the membrane-coated sensor nanoparticles under four conditions: no inhibitor (blue), a constant concentration (0.05 μM) of the inhibitors CTZ-*wt* (red) and CTZ-*mut* (green), and a control (black) with no ZipA (Figure 4a). The interaction of FtsZ to ZipA without inhibitor shows a similar K_D value (3.0 ± 0.6 μM) but a notable smaller Hill coefficient value (n = 0.6 ± 0.1) compared to the membrane-free system. In the absence of a precise molecular mechanism to describe the interaction, the negative cooperativity (n < 1) might indicate a different spatial orientation of the receptor protein in the presence of negatively charged lipids. The binding isotherms in the presence of inhibitors are also similar compared to the membrane free system with K_D values of 19.0 ± 6.0 μM (CTZ-*wt*) and 12.4 ± 1.5 μM (CTZ-*mut*), respectively. However, the Hill coefficients are now both smaller than unity: n = 0.4 ± 0.1 (CTZ-*wt*) and n = 0.4 ± 0.3 (CTZ-*mut*).

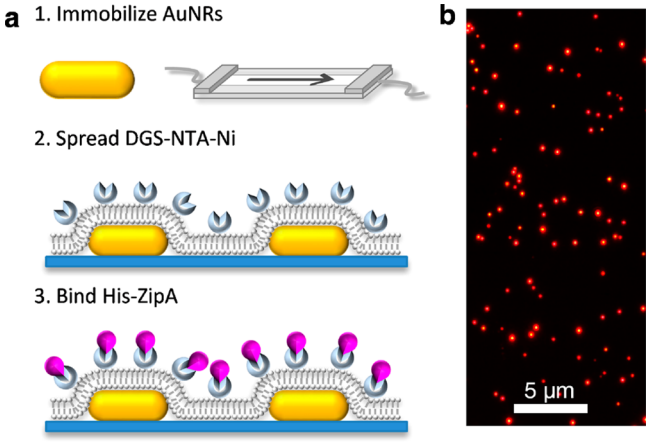

Figure 3. Membrane-coated NanoSPR. (a) Scheme of the strategy to prepare membrane-coated gold nanorods (AuNR) in three steps: (1) nonfunctionalized AuNRs were deposited randomly in a microfluidic flow cell, (2) a lipid membrane containing 10% of DGS-NTA-Ni lipids was spread over the entire surface including the nanoparticles, and (3) the receptor protein ZipA was attached via its His-tag. (b) Real-color dark-field microscope image showing the deposited gold nanorods. Each nanorod serves as a sensing element.

The competition assay with constant ligand concentration (10 μM) and stepwise increasing inhibitor concentration shows qualitatively similar results as before (Figure 4b). However, the effectiveness of inhibition by the two different peptides is reversed compared to the system without membrane: The mutant peptide, in the presence of the lipid membrane, is more effective than the wild type, IC_{50} = 1.8 ± 0.2 μM (CTZ-*wt*) and IC_{50} = 0.6 ± 0.2 μM (CTZ-*mut*). These results agree with previous literature reports (10.9 and 1.6 μM, respectively)[19] where the effect could be attributed to the negatively charged membrane evidenced by the close interaction of FtsZ-ZipA complexes with lipid membranes.[25,26] A schematic representation of the competitive inhibition is represented in the Figure 5, and all the obtained values are summarized in Table 1. In our

DOI: 10.1021/acsami.6b14013
ACS Appl. Mater. Interfaces 2017, 9, 218−223

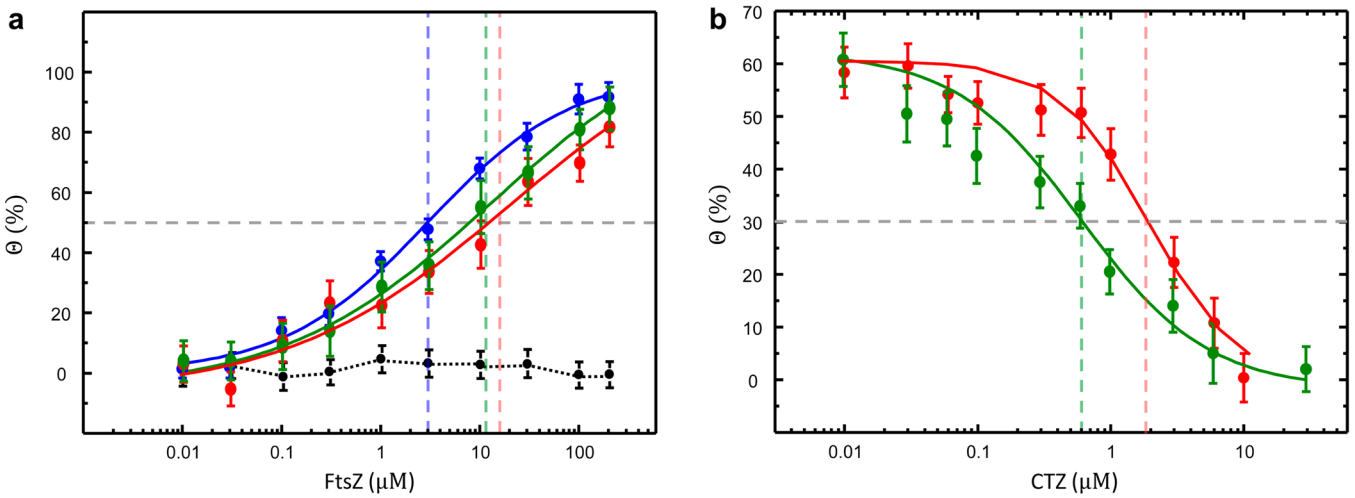

Figure 4. Binding isotherms and competition assay for membrane coated particles. (a) Binding isotherms of the ligand FtsZ to ZipA on the membrane-coated nanosensors (blue). The binding isotherms of FtsZ to membrane bound-ZipA shift to higher concentrations (lower affinity) in the presence of the inhibitor peptides CTZ-*wt* (red) and CTZ-*mut* (green). The control particles show no unspecific interaction with FtsZ (black). (b) For the competition assays in the presence of the membrane, we increase (titrate) the concentration of the inhibitor peptide CTZ-*wt* (red) and CTZ-*mut* (green) keeping the concentration of FtsZ constant (10 μM). This FtsZ concentration corresponds to approximately 65% of the maximum sensor coverage. The dashed lines correspond to the IC_{50} values.

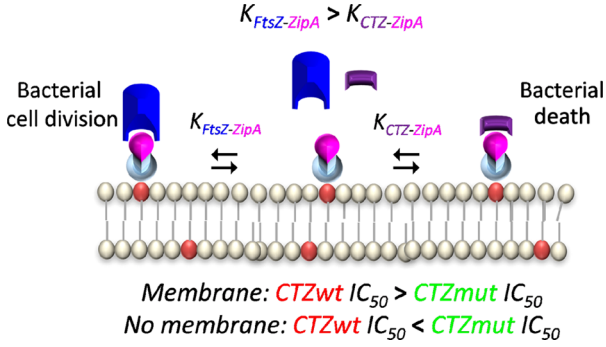

Figure 5. Schematic representation of the inhibition process. The affinity of the inhibitor peptide for ZipA in both cases is stronger than the interaction between FtsZ and ZipA. In the presence of the lipid membrane, the mutant inhibitor is more effective than the *wild type*.

example, the effectiveness of the drug would drive the process to bacterial death by stopping the bacterial cell division process.

With the setup configuration and the nanorods used in this work, we have a detection limit of around 1 nM and a few kDa. To improve the detection limits and detect and quantify the binding of the inhibitor molecules (around 1 kDa), we could use smaller nanorods and more intense light sources like a laser. Stronger illumination increases the temperature of the nanoparticles, but it should be possible to keep this temperature increase below 1−2 K in most cases.[14,20,27]

Table 1. K_D, *n*, and IC_{50} Values Obtained in This Work by NanoSPR

Membrane	Interaction	K_D (μM)	*n*	IC_{50}
-	ZipA-FtsZ	5.3 ± 0.5	1.0 ± 0.1	
+		3.0 ± 0.6	0.6 ± 0.1	
-	ZipA-FtsZ + CTZmut	25.2 ± 3.0	1.7 ± 0.3	2.0 ± 0.4
+		12.4 ± 1.5	0.4 ± 0.3	0.6 ± 0.2
-	ZipA-FtsZ + CTZwt	33.0 ± 6.1	2.0 ± 0.6	0.8 ± 0.2
+		19.0 ± 6.0	0.4 ± 0.1	1.8 ± 0.2

3. CONCLUSIONS

Using NanoSPR, we have quantified the interaction between FtsZ and ZipA and two inhibitors (CTZ-*wt* and CTZ-*mut*) in the presence and absence of an artificial membrane mimicking the bacterial inner membrane. Qualitative similar results were obtained in both cases, but more careful quantitative analysis shows notable differences: differences in the apparent cooperativity between the interacting species (FtsZ and ZipA) induced by presence of the membrane and a reversal of the effectiveness of the inhibitors. One of the tested peptides showed about 1 order of magnitude reduced effectiveness in the membrane environment. This study shows the potential of NanoSPR to provide a simple, fast, and direct route for the quantitative comparison of membrane protein−protein interactions and drug effectiveness. Of special importance is the ability to study receptors embedded in their natural membrane environment, making NanoSPR an interesting tool in pharmaceutical and biomedical laboratories.

4. MATERIALS AND METHODS

Materials. If not stated otherwise, reagents of analytical grade were acquired from Sigma-Aldrich or Merck. Deionized water from a Millipore system (>18 MΩ, Milli Q) was used in all experiments. Isothiocyanobenzyl-NTA was purchased from Dojindo EU GmbH. T-linker-DNA (5′-SH-TTTTTTTTTT-3′) and Thiolated-DNA (5′-SH-TTTTTTTTTT-NH_2-3′) were purchased from Biomers.net GmbH. The proteins were dialyzed in the working buffer (50 mM Tris-HCl pH 7.5, 100 mM KCl, 5 mM $MgCl_2$). For FtsZ, we added 0.05 mM of GDP to the buffer.

Protein Purification. Wild-type FtsZ from *Escherichia coli* was expressed and purified by the calcium-induced precipitation method.[28] The ZipA gene was modified by removing part of the N-terminal domain (amino acids 1−25).[29] After overexpression and purification, FtsZ and ZipA proteins were equilibrated in the working buffer,

DOI: 10.1021/acsami.6b14013
ACS Appl. Mater. Interfaces 2017, 9, 218−223

frozen, and stored at −80 °C in 20 μL aliquots. CTZ-*wt* and CTZ-*mut* were synthesized using traditional solid-phase technology.[6]

Synthesis of Gold Nanorods. A stock of gold nanorods (Au NRs) was synthesized as described in ref 20. Excess surfactant was removed by centrifugation at 2800*g* for 20 min. This procedure was repeated twice, each time the supernatant replaced with 0.05 M CTAB. The nanorods' dimension was determined from TEM images of at least 400 particles resulting in a mean width of 31.1 nm ±5.6 nm and length of 67.8 nm ±9.2 nm (standard deviation, Figure S1).

DNA Stabilization, NTA Functionalization, and His-Tagged Protein Immobilization. The nanoparticle functionalization protocol described in our previous work[10] was subtly modified to exclude the SDS used and increase the coverage of NTA groups. In a typical procedure, 500 μL of CTAB-stabilized gold nanorods was centrifuged at 6300*g* for 5 min. After careful removal of the supernatant, the pellet was resuspended in 50 μL of Milli-Q water and added into 50 μL of chloroform. This immiscible aqueous suspension−chloroform mixture was sonicated for 30 s in order to sequester most of the residual CTAB at the interface between the two solvents. Further, the aqueous phase was recovered, stabilized with 0.01% (v/v) Tween solution and centrifuged again at 6300*g* for 3 min. The pellet was resuspended in a bifunctional DNA solution (consisting of 10 μL of 500 μM thiolated-TTTTTTTTTT-NH2 DNA and 5 μL of 100 mM TCEP dissolved in 35 μL of PBS buffer) and incubated for 3 h under ambient conditions. Later, 2 μL of 10 mg/mL of isothiocyanobenzyl-NTA (dissolved in DMSO) was added to the DNA functionalized nanorods, and the reaction mixture was incubated at room temperature for another 2 h. The resulting NTA-DNA functionalized particles were centrifuged at 6300*g* for 5 min, and the pellet was resuspended in a 50 μL aqueous solution of 100 μM $NiCl_2$ for 10 min (see Figures S2 and S3).

For the protein immobilization, we took 10 μL of the Ni^{2+}-NTA functionalized nanorod stock, centrifuged once at 6300*g* for 5 min, and incubated the pellet in 100 μL of 50 nM His-tag protein (ZipA) solution for 10 min. The excess of unbound protein was left in the solution.

Supported Lipid Membrane. Two separate 0.1 M stock solutions of the lipids *E. coli* polar extract and DGS-NTA(Ni) (Avanti Polar Lipids) were prepared in $CHCl_3/CH_3OH$ 1:1 (v/v) solvent. A mixture of 90% *E. coli* polar extract 10% DGS-NTA(Ni) (mol/mol) was evaporated first under a nitrogen stream and then under vacuum overnight. The dried lipids were resuspended in buffer (50 mM Tris-HCl (pH 7.5), 150 mM NaCl). To obtain small unilamellar vesicles (SUVs), the suspension was sonicated for 10 min at 30 °C. To fuse the lipid bilayer on the sensor substrate, a dilute 0.1 mM solution of the SUVs supplemented with $CaCl_2$ (2 mM) was flushed in the flow cell after the attachment of the AuNRs for 45 min at 30 °C. Then, the flow cell was rinsed with buffer (50 mM Tris-HCl (pH 7.5), 100 mM KCl, 5 mM $MgCl_2$) to remove excess SUVs.

Titration Experiments. To carry out the titration experiments of the interacting partners (FtsZ-ZipA), solutions with concentration from 100 nM to 100−200 μM of FtsZ (in the presence and absence of CTZ-*wt* or CTZ-*mut*, as specified in the main text) were flushed through the flow cell until the sensor response reached an equilibrium value (after about 20 min), so the total time for a complete experiment takes around 3−4 h. We used a flow rate of 30 μL/min, which is high enough to avoid mass transport (diffusion) problems. The experiments were conducted at a constant room temperature of 22 °C. To determine the binding parameters, we used the Hill equation ($\Delta\lambda/\Delta\lambda_{max} = [FtsZ]^n/K_D + [FtsZ]^n$) (with the coverage $\Theta = \Delta\lambda/\Delta\lambda_{max}$) as a fitting function, where $\Delta\lambda_{max}$, n, and K_D are the fitted parameters and $\Delta\lambda$ and [FtsZ] are the known parameters.

Competition Assays. For the competition assays, we first flushed FtsZ (10 μM) into the flow cell. At this concentration of FtsZ, the coverage of ZipA receptors reaches around 65%. In every step of the titration, we used this constant FtsZ concentration while increasing the concentration of the inhibiting peptide from 0.01 to 30−100 μM. All the experiments were conducted at a constant room temperature of 22 °C.

■ ASSOCIATED CONTENT

Supporting Information

The Supporting Information is available free of charge on the ACS Publications website at DOI: 10.1021/acsami.6b14013.

Detailed information on particle characterization and setup improvements (PDF)

■ AUTHOR INFORMATION

Corresponding Authors

*E-mail: rahijado@ucm.es.

*E-mail: soennichsen@uni-mainz.de.

ORCID

Rubén Ahijado-Guzmán: 0000-0002-9863-0443

Author Contributions

The manuscript was written through contributions of all authors. All authors have given approval to the final version of the manuscript.

Notes

The authors declare no competing financial interest.

■ ACKNOWLEDGMENTS

This work was financially supported by the ERC grant 259640 ("SingleSens"). J.P. was financially supported by the graduate school of excellence Materials Science in Mainz. This work was supported by the Spanish government through grant BFU2014-52070-C2-2-P to G.R. We thank to Noelia Ropero and Víctor Hernández-Rocamora for their help and purification of the proteins.

■ REFERENCES

(1) Lipkin, W. The Changing Face of Pathogen Discovery and Surveillance. *Nat. Rev. Microbiol.* **2013**, *11*, 133−141.

(2) Courvalin, P. Why is Antibiotic Resistance a Deadly Emerging Disease? *Clin. Microbiol. Infect.* **2016**, *22*, 405−407.

(3) Baym, M.; Stone, L. K.; Kishony, R. Multidrug Evolutionary Strategies to Reverse Antibiotic Resistance. *Science* **2016**, *351*, aad3292.

(4) Corona, F.; Blanco, P.; Alcalde-Rico, M.; Hernando-Amado, S.; Lira, F.; Bernardini, A.; Sanchez, M. B.; Martinez, J. L. The Analysis of the Antibiotic Resistome Offers New Opportunities for Therapeutic Intervention. *Future Med. Chem.* **2016**, *8*, 1133−1151.

(5) Wang, J.; Gao, L.; Lee, Y. M.; Kalesh, K. A.; Ong, Y. S.; Lim, J.; Jee, J. E.; Sun, H.; Lee, S. S.; Hua, Z. C.; Lin, Q. Target Identification of Natural and Traditional Medicines with Quantitative Chemical Proteomics Approaches. *Pharmacol. Ther.* **2016**, *162*, 10−22.

(6) Hernández-Rocamora, V. M.; Reija, B.; García, C.; Natale, P.; Alfonso, C.; Minton, A. P.; Zorrilla, S.; Rivas, G.; Vicente, M. Dynamic Interaction of the *Escherichia coli* Cell Division ZipA and FtsZ Proteins Evidenced in Nanodiscs. *J. Biol. Chem.* **2012**, *287*, 30097−30104.

(7) Patching, S. G. Surface Plasmon Resonance Spectroscopy for Characterisation of Membrane Protein-Ligand Interactions and its Potential for Drug Discovery. *Biochim. Biophys. Acta, Biomembr.* **2014**, *1838*, 43−55.

(8) Doyle, S. K.; Pop, M. S.; Evans, H. L.; Koehler, A. N. Advances in Discovering Small Molecules to Probe Protein Function in a Systems Context. *Curr. Opin. Chem. Biol.* **2016**, *30*, 28−36.

(9) Wójcik, M.; Telzerow, A.; Quax, W. J.; Boersma, Y. L. High-Throughput Screening in Protein Engineering: Recent Advances and Future Perspectives. *Int. J. Mol. Sci.* **2015**, *16*, 24918−24945.

(10) Ahijado-Guzmán, R.; Prasad, J.; Rosman, C.; Henkel, A.; Tome, L.; Schneider, D.; Rivas, G.; Sönnichsen, C. Plasmonic Nanosensors for Simultaneous Quantification of Multiple Protein-Protein Binding Affinities. *Nano Lett.* **2014**, *14*, 5528−5532.

DOI: 10.1021/acsami.6b14013
ACS Appl. Mater. Interfaces 2017, 9, 218−223

(11) Anker, J. N.; Hall, W. P.; Lyandres, O.; Shah, N. C.; Zhao, J.; Van Duyne, R. P. Biosensing with Plasmonic Nanosensors. *Nat. Mater.* **2008**, *7*, 442−453.
(12) McFarland, A. D.; Van Duyne, R. P. Single Silver Nanoparticles as Real-Time Optical Sensors with Zeptomole Sensitivity. *Nano Lett.* **2003**, *3*, 1057−1062.
(13) Sönnichsen, C.; Franzl, T.; Wilk, T.; von Plessen, G.; Feldmann, J.; Wilson, O.; Mulvaney, P. Drastic Reduction of Plasmon Damping in Gold Nanorods. *Phys. Rev. Lett.* **2002**, *88*, 077402.
(14) Sepúlveda, B.; Angelomé, P. C.; Lechuga, L. M.; Liz-Marzán, L. M. LSPR-Based Nanobiosensors. *Nano Today* **2009**, *4*, 244−251.
(15) Lock, R. L.; Harry, E. J. Cell-division Inhibitors: New Insights for Future Antibiotics. *Nat. Rev. Drug Discovery* **2008**, *7*, 324−338.
(16) Rico, A. I.; Krupka, M.; Vicente, M. In the Beginning, *Escherichia coli* Assembled the Proto-Ring: an Initial Phase of Division. *J. Biol. Chem.* **2013**, *288*, 20830−20836.
(17) Liu, Z.; Mukherjee, A.; Lutkenhaus, J. Recruitment of ZipA to the Division Site by Interaction with FtsZ. *Mol. Microbiol.* **1999**, *31*, 1853−1861.
(18) Mosyak, L.; Zhang, Y.; Glasfeld, E.; Haney, S.; Stahl, M.; Seehra, J.; Somers, W. S. The Bacterial Cell-Division Protein ZipA and its Interaction with an FtsZ Fragment Revealed by X-ray Crystallography. *EMBO J.* **2000**, *19*, 3179−3191.
(19) Kenny, C. H.; Ding, W.; Kelleher, K.; Benard, S.; Dushin, E. G.; Sutherland, A. G.; Mosyak, L.; Kriz, R.; Ellestad, G. Development of a Fluorescence Polarization Assay to Screen for Inhibitors of the FtsZ/ZipA Interaction. *Anal. Biochem.* **2003**, *323*, 224−233.
(20) Rosman, C.; Prasad, J.; Neiser, A.; Henkel, A.; Edgar, J.; Sönnichsen, C. Multiplexed Plasmon Sensor for Rapid Label-Free Analyte Detection. *Nano Lett.* **2013**, *13*, 3243−3247.
(21) Hill, A. V. The Possible Effects of the Aggregation of the Molecules of Hemoglobin on its Dissociation Curves. *J. Physiol.* **1910**, *40*, 190.
(22) Abeliovich, H. An Empirical Extremum Principle for the Hill Coefficient in Ligand-Protein Interactions Showing Negative Cooperativity. *Biophys. J.* **2005**, *89*, 76−79.
(23) Yung-Chi, C.; Prusoff, W. H. Relationship Between the Inhibition Constant (K1) and the Concentration of Inhibitor which Causes 50% Inhibition (I50) of an Enzymatic Reaction. *Biochem. Pharmacol.* **1973**, *22*, 3099−3108.
(24) Hulme, E. C.; Trevethick, M. A. Ligand Binding Assays at Equilibrium: Validation and Interpretation. *Br. J. Pharmacol.* **2010**, *161*, 1219−1237.
(25) Cabré, E. J.; Sánchez-Gorostiaga, A.; Carrara, P.; Ropero, N.; Casanova, M.; Palacios, P.; Stano, P.; Jiménez, M.; Rivas, G.; Vicente, M. Bacterial Division Proteins FtsZ and ZipA Induce Vesicle Shrinkage and Cell Membrane Invagination. *J. Biol. Chem.* **2013**, *288*, 26625−26634.
(26) Loose, M.; Mitchison, T. J. The Bacterial Cell Division Proteins FtsA and FtsZ Self-Organize into Dynamic Cytoskeletal Patterns. *Nat. Cell Biol.* **2014**, *16*, 38−46.
(27) Ament, I.; Prasad, J.; Henkel, A.; Schmachtel, S.; Sönnichsen, C. Single Unlabeled Protein Detection on Individual Plasmonic Nanoparticles. *Nano Lett.* **2012**, *12*, 1092−1095.
(28) Rivas, G.; López, A.; Mingorance, J.; Ferrandiz, M. J.; Zorrilla, S.; Minton, A. P.; Vicente, M.; Andreu, J. M. Magnesium-Induced Linear Self-Association of the FtsZ Bacterial Cell Division Protein Monomer. The Primary Steps for FtsZ Assembly. *J. Biol. Chem.* **2000**, *275*, 11740−11749.
(29) Martos, A.; Alfonso, C.; López-Navajas, P.; Ahijado-Guzmán, R.; Mingorance, J.; Minton, A. P.; Rivas, G. Characterization of Self-Association and Heteroassociation of Bacterial Cell Division Proteins FtsZ and ZipA in Solution by Composition Gradient-Static Light Scattering. *Biochemistry* **2010**, *49*, 10780−10787.

DOI: 10.1021/acsami.6b14013
ACS Appl. Mater. Interfaces 2017, 9, 218−223